

Simulation Study About the Influence of Atmospheric Stratification on Lightning Activities*

ZHENG Dong^{1,2†}(郑栋), ZHANG Yijun^{1,3}(张义军), LU Weitao¹(吕伟涛),
MA Ming¹(马明), and MENG Qing¹(孟青)

¹ *Laboratory of Lightning Physics and Protection Engineering, Chinese Academy of Meteorological Sciences, Beijing 100081*

² *Graduate School of Chinese Academy of Sciences, Beijing 100039*

³ *State Key Laboratory of Severe Weather, Chinese Academy of Meteorological Sciences, Beijing 100081*

(Received November 27, 2007)

ABSTRACT

A 2D model about charging and discharging processes in thundercloud is used to simulate three differential atmospheric stratifications resulting in discrepant thunderstorm processes in Beijing region. The dynamic and microphysical processes in thunderstorm and their influence on lightning activities are also discussed. The results indicate that ascending velocity and water vapor are the most important factors to influence lightning activities. At the same time, they affect each other and are together controlled by atmospheric stratification. The magnitude of the ascending velocity determines the intensity of storm and the time when the thunderstorm matured. The thunderstorm with strong updrafts can reach a large height in a short time. Strong persistent updrafts and sufficient water vapor which help to generate more ice phase hydrometeors that directly influence charging and discharging process will prolong the mature stage of the thunderstorm and thereby enhance lightning activities. Though the big density of ice phase hydrometeors can be formed, it is difficult to sustain a long time in the condition of strong updrafts and scant water vapor. Under the condition of weak updrafts and sufficient water vapor in the whole levels, it is easy to form warm cloud process in which the ice phase process and lightning activities are weak. The favorable stratification conditions for strong lightning activities are the sufficient vapor in the lower atmosphere, moderate humidity in the mid troposphere, big instability energy and some suitable convective inhibition. Through calculating some atmospheric instability parameters, it is indicated that convective instability index smaller than -10°C (negative means unstable), convective available potential energy larger than 1000 J kg^{-1} , convective inhibition larger than 40 J kg^{-1} , the 700-hPa potential equivalent temperature larger than 340 K and the 35%–85% humidity in the mid troposphere (700–400 hPa) are the advantageous conditions for strong lightning activities.

Key words: atmospheric instability parameters, model, hydrometeor, electric structure

1. Introduction

Atmospheric stratification influences the lightning activities by controlling the dynamic and microphysical processes in thunderstorms. In the research on tropical oceanic thunderstorms, Zipser (1994) and Petersen et al. (1996) pointed out that lightning activities occurred only when the ascending velocity at the -10°C level reached $6\text{--}7\text{ m s}^{-1}$. Colson (1960) found that the lightning activities would be frequent when the atmospheric instability and rainfall were strong. Rutledge et al. (1992), Williams et al. (1992), Randell et al. (1994), and Petersen et al. (1996) had found

that strong lightning activities are associated with big convective available potential energy (CAPE). However, Williams et al. (1992) also pointed out that some other atmospheric instability indices also affected the lightning frequency. Yuan and Qie (2005) noted there was a close relationship between sensible heat flux or Bowen ratio and lightning activities in the central Tibetan Plateau. Through model analysis, Guo et al. (2003, 2004) believed that CAPE and the average relative humidity in middle levels were very important indices affecting lightning activities. Under different conditions of atmospheric stratification, obvious differences about electric structures were found.

*Supported by the National Natural Science Foundation of China under Grant Nos. 40475002 and 40605004, the National Basic Research Program of China under No. 2004CB418306, and the Dean Fund of Chinese Academy of Meteorological Sciences.

[†]Corresponding author: zhd@cams.cma.gov.cn.

Qie et al. (2005) also found from model analysis that reversal temperature and the average relative humidity in the mid level played a vital role in forming electric structures of thunderstorm. Comparing with the simulation results of thunderstorms in the different areas of China, Zhang et al. (2000) indicated that the height range from -10 to -20°C is an important parameter for lightning activities. In addition, the stratification in the northern China is advantageous for tripole electric structure. Yan et al. (1996a, b) found that lightning activities depended on the thermal dynamic characteristics near the cloud base to a large extent. Strong charging process occurred only when the strong updrafts ascended through the height of -20°C . Furthermore, strong lightning activities usually took place when the maximum ascending velocity was descending. Sun et al. (2002) found that the occurrence of ice phase particle would strengthen charging process. Ma (2004) used a 2D charging and discharging model in thunderstorms to discuss the difference of lightning activities between hail storms and rain storms in different atmospheric stratifications.

In this paper, the model developed by Ma (2005) is used to simulate three different atmospheric stratifications resulting in discrepant thunderstorm processes in Beijing region. Furthermore, how stratification and atmospheric instability parameters affect lightning activities is discussed. The model was developed by adding charging and discharging process into the original 2D cumulonimbus model developed by Hu and He (1987), Wang and Hu (1990), and Yu et al. (2001). Gardiner's parameterization project (Gardiner et al., 1985) was adopted to parameterize main non-inductive charging (NIC) mechanism, and Mansell's parameterization project of stochastic lightning (Mansell et al., 2002) was adopted to parameterize the lightning discharging process. The spatial domain of the model was a 76-km length and 20-km height with every grid length 1 km and grid height 0.5 km, respectively. Time step separation in the model was used with a big time step of 4 s and a small time step of 2 s. The model test proved its good analysis performance.

2. Definition of atmospheric instability parameters

Zheng et al. (2005) analyzed the relationship between lightning activities and instability parameters in Beijing region and found that the average relative humidity between 700 and 400 hPa, CAPE, lifted index, 700-hPa potential equivalent temperature, latent instability index, and convective instability index are all warning parameters of lightning activities. These parameters are used in this paper and their simple explanations are shown as follows.

Average relative humidity between 700 and 400 hPa ($U_{w700-400}$): Because the air between 700 and 400 hPa is corresponding to the mid-troposphere at heights of 3–7.5 km where usually is the major formation range of thunderstorms in Beijing, the condition of its water vapor is of an important impact on dynamic, microphysical, and electrification processes in thunderstorms.

Convective available potential energy (CAPE): The equation of CAPE can refer to the paper (Zheng et al., 2005). The CAPE indicates that the size of instability energy is proportional to the positive area between sounding line and parcel line in $T\text{-ln}p$ graph. The difference between equilibrium altitude (EA) and level of free convective (LFC) expresses the thickness of instability energy. The difference between sounding line and parcel line, furthermore, expresses the size of the buoyancy.

Convective inhibition (CIN): The equation of CIN can refer to the paper (Zheng et al., 2005). The CIN indicates that the magnitude of energy restraining convection is proportional to the negative area between sounding line and parcel line in the underlayer of $T\text{-ln}p$ graph.

Lifted index (LI): It is defined to be the difference between sounding temperature and the parcel temperature at 500-hPa level and expresses the size of buoyancy at 500 hPa.

The 700-hPa potential equivalent temperature (θ_e): It expresses the temperature a parcel should have

when the parcel is lifted to the condensation level through dry adiabatic process, then lifted to a high level where the water vapor is close to 0 through pseudo moist-adiabatic process and finally descends to the 1000-hPa level through dry adiabatic process. The θ_e synthetically presents the condition of temperature and humidity at 700-hPa level. Large θ_e is related to high temperature and humidity. The 700-hPa level is chosen because there exist air current convergence and obvious characteristics of temperature and humidity in the base of the cloud.

Latent instability index (I_L): The definition can refer to the papers (Zheng et al., 2005; Wu and Wang, 1987). The atmospheric stratification is unstable when I_L is smaller than 0, which means there are high temperature and high humidity on the ground and low temperature at 500 hPa.

Convective instability index (I_C): The definition can refer to the papers (Zheng et al., 2005; Wu and Wang, 1987). The atmospheric stratification is unstable when the value of I_C is smaller than 0, which means

there are high temperature and humidity at 850 hPa but at the same time there are low temperature and low humidity at 500 hPa.

3. Choice of atmospheric stratification

According to the characteristics of stratification, the actual strength of lightning activities and simulative results, three different soundings in Beijing are chosen and input to the model with the same initial startup conditions. The results are shown in Table 1. Cloud-to-ground lightning discharges were observed by M-LDARS (Zheng et al., 2005). It must be emphasized that because of the immature simulation technology at present, the simulative lightning number is usually less than the actual lightning number. Table 1 shows that different characteristics exist among the three soundings, which will be expounded in Section 4. Simply three soundings and their weather processes are respectively named Processes 1, 2, and 3 in the following analysis.

Table 1. Atmospheric instability parameters of three different weather processes and some simulation results

Parameters and part of simulation results	Sounding 1 1997-07-28 0800BT (Beijing Time)	Sounding 2 1997-07-22 0800BT	Sounding 3 1996-07-29 0800BT
$U_{w700-400}$ (%)	40.21	22.40	80.94
I_L (°C)	-4.80	-12.07	-6.34
I_C (°C)	-13.80	-15.72	-1.47
CAPE(J kg ⁻¹)	1243.27	3362.83	1384.00
CIN(J kg ⁻¹)	42.63	22.87	3.92
LI (°C)	-2.50	-5.64	-3.23
θ_e (K)	341.33	332.55	340.29
Cloud top height (km)	14.89	17.36	14.55
Maximal ascending velocity (m s ⁻¹)	29.93	44.40	14.05
Height of 0°C level (km)	5.25	5.28	5.07
Height of -10°C level (km)	7.01	6.68	7.00
Height of -20°C level (km)	8.61	8.00	8.59
Cloud-to-ground lightning number observed by M-LDARS	1999	66	301
Simulative lightning number	164	10	44
Simulative electric structure	tripolar	dipolar→tripolar→dipolar	tripolar

4. Analysis of simulative results

4.1 Process 1

The sounding line, parcel line, and dew point line of Process 1 are plotted in Fig.1a. The $U_{w700-400}$ value

of 40.21% means the moderate water vapor condition in the middle level. LFC is near 800-hPa level and EA is near 200-hPa level, which means the thick layer of instability. CAPE is large with the value being 1243.27 J kg⁻¹. The values of LI and θ_e are -2.50°C and

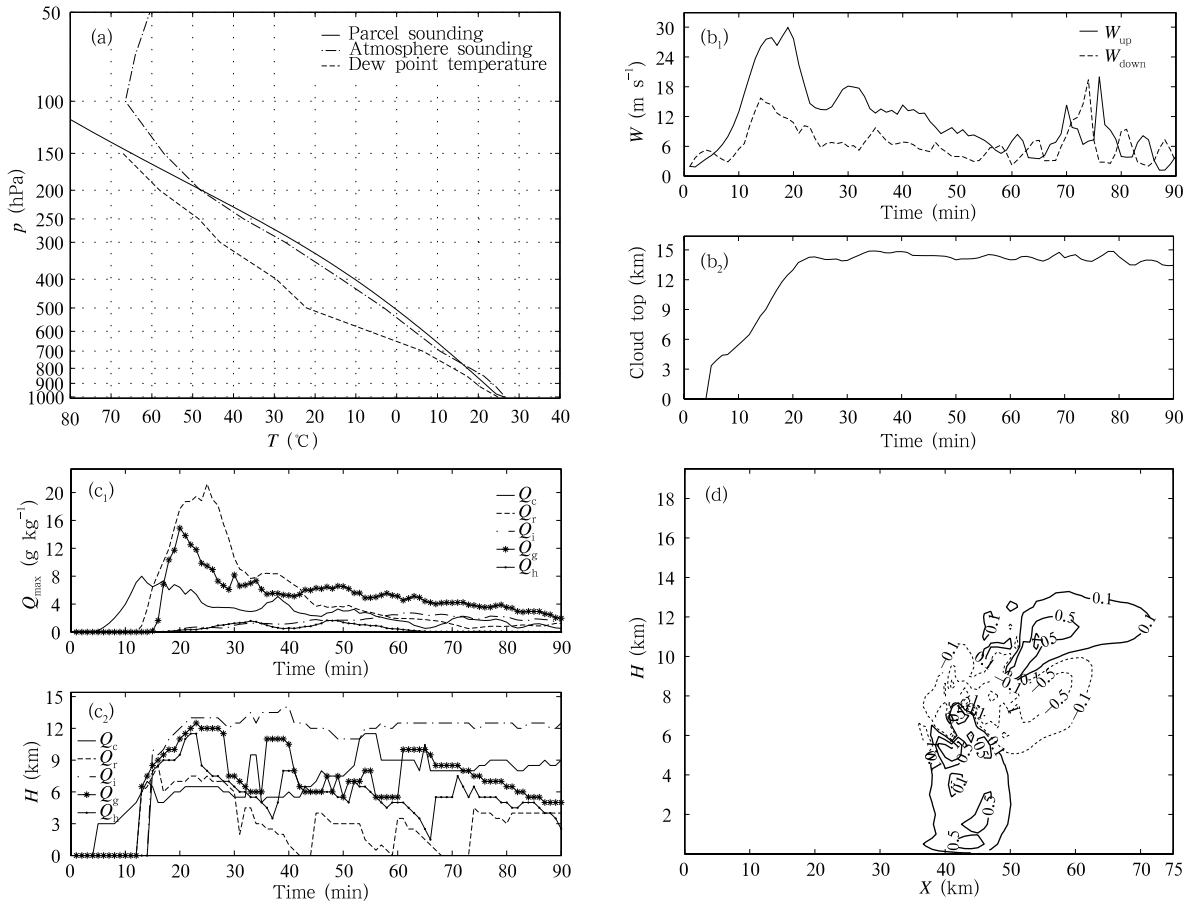


Fig.1. The stratification characteristics and simulation results for Process 1. (a) Stratification characteristics (“- · -”: sounding, “- -”: dew point, “—”: parcel state), (b) change of maximum ascending velocity W_{up} , maximal falling velocity W_{down} , and maximal cloud top height, (c) maximum mass proportion of various hydrometeors and their change with height (subscript c: cloud droplet, r: rain droplet, i: ice crystal, g: graupel, and h: hail), and (d) charge structure at the 51st minute (“—”: positive charge, “- - -”: negative charge).

341.33 K, respectively, which also mean the instable stratification. In addition, there is high humidity at 700 hPa. The I_L value of $-4.08^\circ C$ means that latent instability is not strong. Convective instability is strong with the value being $-13.80^\circ C$ due to the enough water vapor at 850 hPa and low humidity at 500 hPa.

Figure 1b shows the temporal variations of the maximum ascending velocity, the maximum falling velocity, and the cloud top height (CTH). The maximum ascending velocity appears at the 19th minute of simulation time with a value of $29.93 m s^{-1}$ and the maximum falling velocity appears at the 14th minute with a

value of $15.71 m s^{-1}$. After the maximum values, they rapidly decline to about 14 and $7 m s^{-1}$, respectively, and then the downward trends become gentle. Before the 60th minute, the ascending velocity dominates in a general way with a maximum value about $10 m s^{-1}$, and after the 60th minute, it becomes equivalent with the falling velocity. CTH reaches its maximum value (14.89 km) at the 35th minute and additionally keeps about 14 km after the 23rd minute. The reason is that strong ascending velocity sustaining for a long time and favorable humidity in the middle and low levels (it refers to the atmosphere below 700 hPa in this paper) provide with sufficient water vapor for the

microphysical process in the cloud, which also results in the long mature duration of the cloud.

The temporal variations in the maximum mass proportion and its height of five kinds of hydrometeors including cloud droplet, rain droplet, ice crystal, graupel, and hail are shown in Fig.1c. Under the action of lifting and cooling, the maximum mass proportion of rain droplet located in the region where the height is larger than 6 km and the temperature is lower than 0°C increases and reaches a maximum value (8.00 g kg^{-1}) at the 13rd minute, and then begins to decrease because of the generation of rain droplet, graupel and ice crystal. With the condensation and collection processes, the mass proportion of the rain droplet increases rapidly and reaches its maximum value (21.25 g kg^{-1}) at the 25th minute, and then decreases steadily. The height of the rain droplet is low because of its sedimentation. More graupel particles are produced because the ice crystal particles grow up through collection and congelation with supercooled water droplets located in the region where the temperature is lower than 0°C to form graupel, i.e., riming mechanism (Sheng et al., 2003). After reaching its maximum value (14.89 g kg^{-1}) at the 20th minute, the mass proportion of graupel starts to decrease rapidly with the decreasing ascending velocity, and then changes steadily with the persistence of updrafts and sufficient water vapor supply. The height of the main graupel is larger than 6 km. When the mass proportion of the graupel starts to decrease, the mass proportion of the ice crystal starts to increase slowly with the decreasing ascending velocity, then reaches its maximum value (2.73 g kg^{-1}) at the 62nd minute, and furthermore maintains larger than 1.5 g kg^{-1} all along with the height maintaining larger than 12 km, which is also an important substance reason for the CTH keeping and changing steadily.

Figure 1d shows the tripolar electric structure at the 51st minute. Large charge density (definition: the absolute value of charge density is larger than 1 nC m^{-3}) appears from the 34th to 82nd minute. The height of the upper main positive charge region is larger than 10 km and maximum positive charge

density center is located at the height of about 12 km where the temperature is lower than -30°C . The height of the middle main negative charge is between 6 and 10 km where the temperature is lower than -10°C . The maximum negative charge density center is located at the height of about 8 km where the temperature is lower than -15°C . Under the action of NIC mechanism, graupel and hail particles in the region where the temperature is lower than the reversal temperature -15°C (Ziegler and MacGorman, 1994) carry negative charge and the ice crystal particles carry positive charge with suitable water vapor condition. Because of the difference of individual weight, the ice phase particles separate under the action of updraft. The ice crystal particles carrying positive charge are lifted to the upside and form the upper positive charge region while the graupel and hail particles taking negative charge stay behind and form the middle negative charge region. In addition, there is also a positive charge region under the height of 6 km. The graupel and hail particles in the region with a temperature higher than the reversal temperature carry positive charge through NIC mechanism, which leads to the electrical field positive. Through inductive charging mechanism, the small cloud droplets transported to the region with a temperature lower than -15°C by the updrafts carrying negative charge and the falling water droplets carrying positive charge, which make the main contribution to the bottom positive charge region. The lightning activities in Process 1 are the strongest among the three processes with 164 lightning discharges being simulated and 1999 cloud-to-ground lightning discharges being detected.

In summary, the convection in Process 1 is strong and can persist for a long time. Furthermore, the water vapor at middle levels is suitable and the water vapor condition at middle and low levels is good. That the updrafts carry sufficient water vapor to the region with a temperature lower than 0°C is in favor of the generation of all kinds of ice phase particles and charging process which leads to larger charge density and strong charge field in cloud. Therefore simulative and actual lightning activities are both active.

4.2 Process 2

Figure 2a shows that the water vapor content in the middle level is low with the value of $U_{w700-400}$ being only 22.04%. That the LFC is near to 700 hPa and EL is near to 150 hPa indicates a large instability thickness. The value of CAPE being 3362.83 J kg^{-1} indicates very large instable energy. The value of CIN is 22.87 J kg^{-1} . The value of LI is -5.64°C , which indicates the large buoyancy at 500 hPa. The reason why θ_e with the value being 332.55 K is smaller than that in Process 1 maybe is that the humidity at 700-hPa level is small in this process. Latent instability and convective instability are both strong with the value being -12.07 and -15.72°C , respectively under

the conditions of high temperature and humidity at 850 hPa and the very low humidity at 500-hPa level.

Figure 2b shows that the ascending velocity reaches 44.40 m s^{-1} at the 27th minute, which is maximum among the three processes and the falling velocity reaches its maximum value (18.05 m s^{-1}) at the 26th minute. After that, they both decrease rapidly and the trend changes to be gentle after the 40th minute. The maximum CTH reaches 17.36 km which is the largest among the three processes at the 30th minute under the action of very strong updrafts, and then starts to decrease with a falling trend accelerating after the 70th minute.

From Fig.2c, it is clear that the mass proportion of cloud droplet, rain droplet, graupel and ice crystal

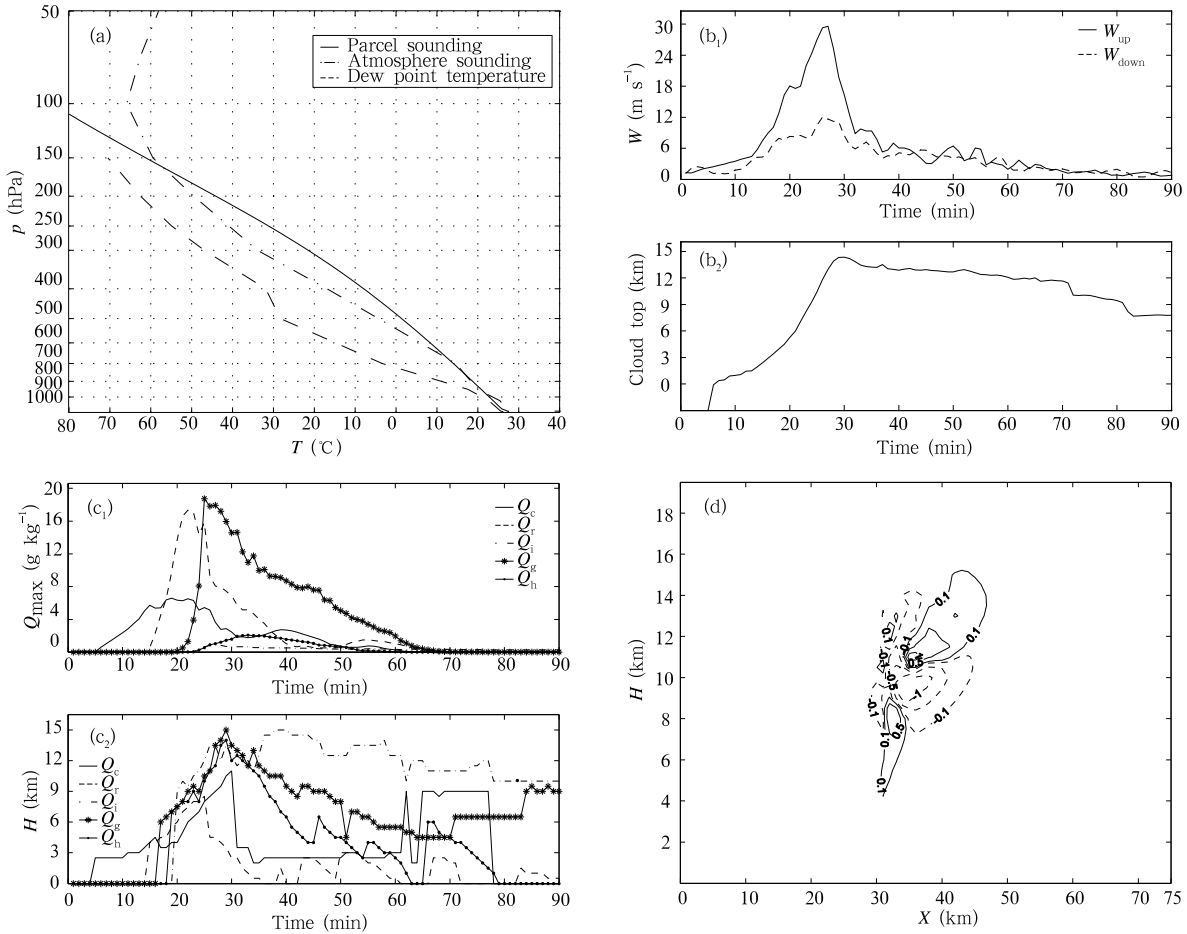


Fig.2. The stratification characteristics and simulation results for Process 2. (a) Stratification characteristics, (b) change of maximum ascending velocity, maximum falling velocity, and maximum cloud top height, (c) maximum mass proportion of various hydrometeors and their change with height, and (d) charge structure at the 35th minute.

increases in turn with the maximum value being 6.57 g kg^{-1} at the 19th minute, 17.33 g kg^{-1} at the 22nd minute, 17.91 g kg^{-1} at the 27th minute, and 0.88 g kg^{-1} at the 27th minute, respectively. Obviously, the maximum mass proportions of the cloud droplet and the rain droplet are smaller than those in Process 1. But the maximum mass proportion of the graupel is larger than that in Process 1. It is because that the water vapor supply in Process 2 is not so sufficient as Process 1, which decreases the mass proportion of cloud droplet and rain droplet. At the same time, because of the prior strong updraft lifting the ice crystal and the supercooled water to a larger height and accelerating the collision and congelation process, the maximum mass proportion of the graupel is very large and the height during the vigorous stage is larger than that in Process 1. But with the rapid decrease of the ascending velocity and the insufficient water vapor condition, the mass proportion of the graupel decreases rapidly and tends to 0 after the 65th minute. For the same reason, the mass proportion of the ice crystal is smaller than that in Process 1 and decreases rapidly. After the 60th minute, the mass proportion of five kinds of hydrometeors all tends to be near 0, which indicates that though there are strong updrafts and instability energy, the dry stratification restrains the generation and persistence of the hydrometeors and furthermore leads to the weak charging process.

During the simulation time, the electric structure is tripolar from the 29th to 46th minute and dipolar in other time. Figure 2d shows the electric structure at the 35th minute. The time of large charge density occurs from the 26th to 52nd minute. Considering the whole simulation process, the density values of the positive and negative charge are both smaller than those in Process 1. Compared with other two processes, the lightning activities in Process 2 are the weakest with only 10 lightning discharges being simulated and 66 cloud-to-ground lightning discharges being detected.

Summarily, though there are very great instability energy, convective instability, strong updrafts, and large maximum CTH in Process 2, the unfavorable water vapor condition in middle levels makes it weak for

the generation of the hydrometeors and the charging process, and along with this, the lightning activities are not active with small charge density and electric field.

4.3 Process 3

From Fig.3a, it is clear that the water vapor between the ground and 150-hPa level is very plenteous with the value of $U_{w700-400}$, 80.94%, which is much larger than that in Processes 1 and 2. The instability energy is thick with the LFC being near 800 hPa and EL being near 200 hPa. CAPE reaches $1384.00 \text{ J kg}^{-1}$, LI is -3.23°C , and the value of θ_e is 340.29 K. CIN is small with the value only being 3.92 J kg^{-1} , which is an important factor that leads latent instability to be a little stronger than that in Process 1 with the value of -6.34°C . Because the humidity at 500 hPa is large, the value of I_C is only -1.47°C .

After reaching their maximum values 14.05 m s^{-1} at the 17th minute and 7.76 m s^{-1} at the 20th minute, respectively (Fig.3b), both the ascending and falling velocities decrease rapidly. The ascending velocity smaller than that in Process 1 dominates the cloud until it is close to the falling velocity with the value about 3 m s^{-1} after the 45th minute, which makes the cloud develop slowly. The main reason why the CTH keeps after reaching its maximum height 14.49 km at the 76th minute is that the hydrometeors continuously generated under the ample water vapor condition are slowly dragged to the upper level by the weak but sustaining updrafts.

Figure 3c shows that the growth order of the mass proportion of five kinds of hydrometeors is the same in Processes 1 and 2. After the mass proportion of cloud droplet reaching its maximum value 6.16 g kg^{-1} at the 19th minute, the rain droplet starts to grow with the collection of the cloud droplet and reaches a maximum value 15.06 g kg^{-1} at the 25th minute. Because of the ample water vapor, the mass proportion of the cloud droplet decreases slowly after the 30th minute and keeps large value in the whole process. Though small ascending velocity makes the growth of the graupel and the hail slow, the sufficient water vapor and

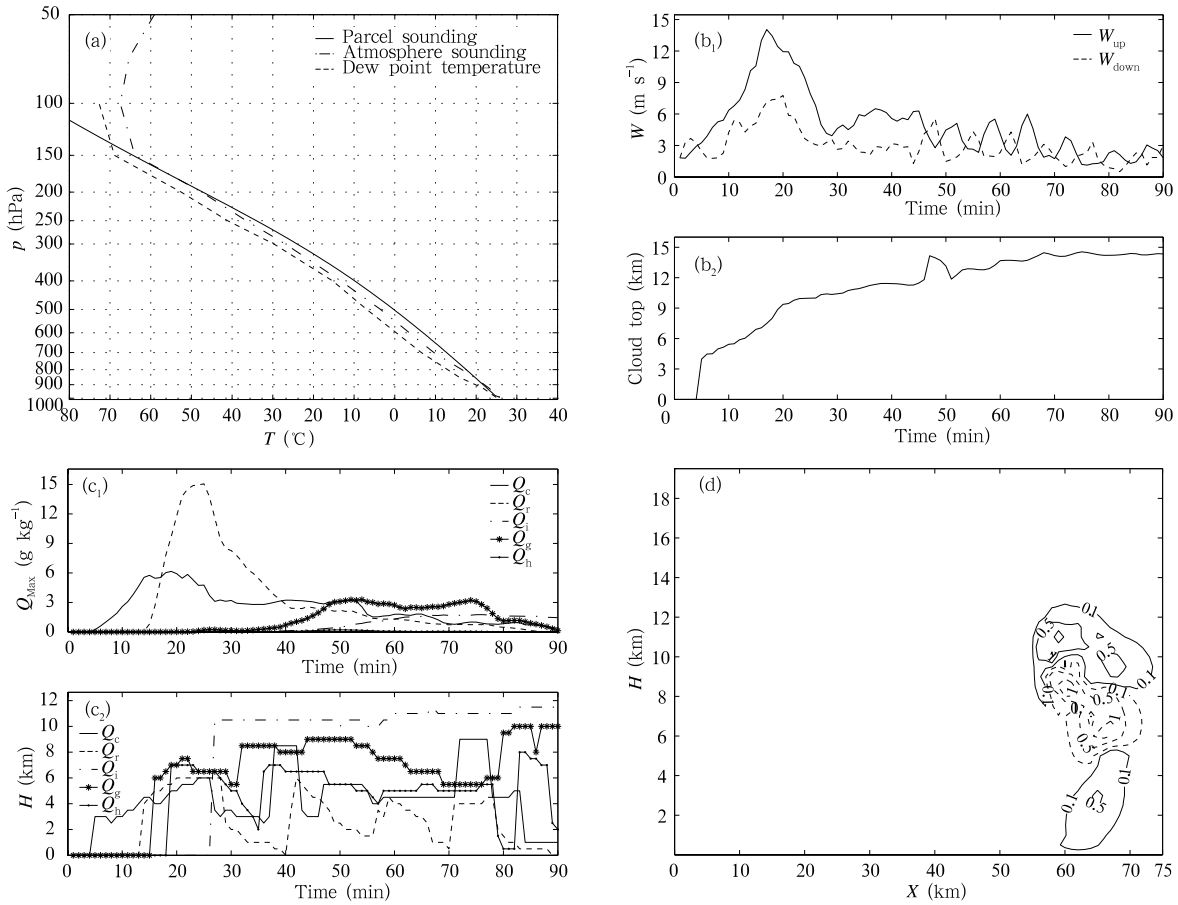


Fig.3. The stratification characteristics and simulation results for Process 3. (a) Stratification characteristics, (b) change of maximum ascending velocity, maximum falling velocity, and maximum cloud top height, (c) maximum mass proportion of various hydrometeors and their change with height, and (d) charge structure at the 66th minute.

the sustaining updrafts make them vary steadily after their maximum values. The average mass proportion of the hydrometeors is smaller than that in Process 1. Furthermore, the mass proportion of the hail which is difficult to be generated but easy to fall with the weak updrafts is always very small.

The electric structure at the 66th minute is shown in Fig.3d. The charging process is slow because of the weak ascending velocity. Strong charge density sustains from the 53rd to 88th minute. After the 50th minute, the positive charge density of which the maximum height is at 11 km starts to increase rapidly with the growth of the ice crystal. Negative charges are mainly distributed in the region between heights of 5 and 10 km. At the same time, there is a weak positive

charge region in the lower part of the cloud. Total 44 lightning discharges are simulated and 301 cloud-to-ground lightning discharges are detected in Process 3.

In summary, there are ample water vapor and large instability energy in Process 3. But the convective instability and the ascending velocity are weak, which results in the slow development of the cloud. The CTH, however, is able to sustain because of the enough water vapor and the sustaining updrafts. The affection of the updrafts and the water vapor condition on the mass proportion and its variation of the rain droplet, the graupel and the ice crystal is remarkable. The small ascending velocity causes the cloud droplets to form the falling rain droplets through collection process before the cloud droplet is consumed to produce

the ice phase hydrometeors, which leads to the small mass proportion of graupel and hail. However, the sufficient water vapor can sustain the hydrometeors to be generated continuously, so that the lightning activity in this process is stronger than that in Process 2.

5. Comparison and discussion of the results

Firstly, the CTH and its persistence are concerned. The CTH in Process 2 is the largest among the three processes due to the maximum ascending velocity. However, because its stratification is dry, the water vapor can only be supplied from the lower atmosphere. With the decrease of the ascending velocity, it is difficult for the water vapor to be transported to the upper level, which restrains the generation of the hydrometeors, so that the CTH decreases with time obviously. Compared with Process 2, the maximum ascending velocity in Processes 1 and 3 is smaller and the values of CTH are both about 14 km. These facts indicate that there is a close relationship between the maximum CTH and the maximum ascending velocity. There is also a difference between Processes 1 and 3. Although the ascending velocity in Process 1 is larger than that in Process 3, the water vapor in the middle level in Process 1 is not as enough as that in Process 3. Under the action of strong updrafts, Process 1 reaches its maximum CTH immediately. Furthermore, because the updraft persists for a long time and the water vapor in the middle and low levels can be supplied to the upper level, the CTH in Process 1 changes little after reaching its maximum height, which helps to prolong the life of the storm and producing more lightning discharges. In Process 3, the weak updraft leads the cloud to reach its maximum height later, but the persisting updraft and the sufficient water vapor make the CTH steady. It is clear that the time when the storm reaches its maximum CTH is affected by the ascending velocity, and whether the CTH can persist or not is determined by the ascending velocity and the water vapor condition commonly.

There is also a close relationship among the change of mass proportion of hydrometeors, ascending velocity, and water vapor. Through the comparison among the three processes, it is found that the rela-

tive maximum mass proportion (compared with own other hydrometeors) of the rain droplet in Process 3 is the largest among all the processes and Process 1 is the second. At the same time the hydrometeor with the relative maximum mass proportion in Process 2 is graupel. Compared with Process 2, there is more sufficient water vapor in Processes 1 and 3, especially in Process 3, and furthermore, the ascending velocity in Processes 1 and 3 is smaller than that in Process 2. Therefore, it is difficult for the cloud droplet and the rain droplet in Processes 1 and 3 to be lifted to the upper level and form ice phase hydrometeors. On the contrary, a considerable amount of water vapor is changed to form rain droplets in the low level and they fall down because the weak updraft cannot lift them. It is also obvious that there is a close relationship between maximum mass proportion of graupel and ascending velocity. Though the condition of water vapor is disadvantageous, the mass proportion of the graupel in Process 2 is the largest in the three processes due to the strongest ascending velocity. The reason is that strong updrafts can lift rain droplets to higher cloud region and accelerate the collection process between ice phase hydrometeors and supercooled water to form graupel. Change in the mass proportion of graupel, however, is related with water vapor. Enough water vapor is in favor of the mass proportion of graupel persisting steadily, such as that in Processes 1 and 3. In Process 2 the stratification is very dry, the mass proportion of graupel rapidly decreases to nearly zero with the decrease of the ascending velocity. The mass proportion of the ice crystal commonly starts to increase when the mass proportion of the graupel starts to decrease. The relationship is also close among maximum mass proportion or the change of mass proportion, the condition of ascending velocity, and water vapor in the middle level. The time when the maximum mass proportion appears is subjected to ascending velocity to a certain extent. Whether the mass proportion of ice crystal can persist depends on whether water vapor supply is enough. The ice crystal in Processes 1 and 3 can persist for a long time because of the good water vapor condition. Analysis also shows that the average value of the mass proportion of ice

phase hydrometeors is determined by ascending velocity and water vapor. Although the water vapor in middle levels in Process 3 is larger than that in Process 1, the absolute and average values of the mass proportion of the graupel and the ice crystal in Process 3 are smaller than those in Process 1, because small ascending velocity makes it difficult for liquid water to be rapidly lifted to the cold upper air (Gunn and Kinzer, 1949; Jorgensen and LeMone, 1989), which leads to the mass proportion of the rain droplet in Process 3 being larger than that in Process 1 after reaching its maximum value and the mass proportion values of the ice phase hydrometeors, however, are smaller than those in Process 1. At the same time, because of the dry stratification, the average mass proportion of the hydrometeors in Process 2 is the smallest among the three processes.

Secondly, charge density and electric structure are concerned. The average charge density in Process 3 is the largest among the three processes and that in Process 2 is the smallest. When ice crystal collides with graupel, the temperature difference between warm frosting surface of graupel and cold frosting surface of ice crystal leads the charge to be transferred under the action of NIC mechanism which is affected by temperature, local supersaturation, supercooled liquid water content, and the size of ice crystal. In Process 1, the average mass proportion of the ice phase hydrometeors is the largest. Furthermore, the strong ascending velocity cannot only accelerate the collision between ice crystal and graupel but also transfer more water vapor to the upper level. It is shown that the height of the maximum mass proportion of the cloud droplet in Process 1 is higher than 9 km for a long time, which is in favor of strong non-inductive charging and forming large charge density. In addition, under the action of strongly electrical field, a strongly inductive positive charge region is formed in the lower cloud. Although the ascending velocity is transitorily large in Process 2, the small mass proportion of the hydrometeors and the liquid water content in the supercooled region make the charging process weak. At the same time, the inductive positive charge region in the lower cloud is very small and persists for a short time due to

the small mass proportion of the rain droplet lifted by the updraft in the lower cloud. The average mass proportion of the graupel and the ice crystal is smaller than that in Process 1, and additionally, the supercooled liquid water content in the region with graupels and ice crystals mixed is also small, both make the charging process in Process 3 weaker than that in Process 1. Process 3 is like a warm cloud process.

Through the previous analysis, it is found that the direct factors affecting the development of storms, generation of hydrometeors, and lightning activities are ascending velocity and water vapor. In the following, the relationship between stratification and lightning activities will be discussed.

It is found that there is a negative relationship between maximum ascending velocity and I_C in the three processes. Small I_C (negative value indicates instability) is usually corresponding with large ascending velocity. Small I_C is associated with large humidity in lower levels and small humidity in middle levels, and therefore large humidity in middle levels is not in favor of strong updrafts (Watson, 1991). Zheng et al. (2005) found that more than 80% of the lightning weather appeared when the humidity in middle levels is between 35% and 85%. The same conclusion was also pointed out by Zhang (1980). Therefore, suitable water vapor in middle levels is an important condition for strong lightning activities. At the same time, it is emphasized that I_C is not the unique factor affecting lightning activities and the combination of CAPE and CIN is another important factor. CAPE expressing instability energy is an indispensable condition for thermal convection. Large CIN implies the extent restraining convection is large, which will make thermal convection difficult to develop. On the contrary, if CIN is too small, it will be difficult for energy to be accumulated in the lower level and the adjustment of convection is easy, which will be disadvantageous to strong convection. Therefore a suitable value for CIN is necessary. It can be found that CAPE in Process 3 is near to that in Process 1, but CIN is smaller than that in Process 1. Correspondingly, the convective activity in Process 3 is not stronger than that in Process 1. Latent instability index (I_L) reflects the relationship

between CAPE and CIN to a certain extent, however, the complicity of the cooperation between CAPE and CIN makes the relationship between I_L and ascending velocity unclear.

Sustained updrafts are of important influence on the generation of hydrometeors and the persistence of storms. According to the simulation analysis, sustained updrafts are influenced by two factors, one is CAPE, and the other is water vapor condition. In Process 1, because the water vapor in middle levels is suitable, that in low levels is sufficient, and CAPE is large, the ascending velocity can be sustained at about 6 m s^{-1} for a long time after its maximum value. In Process 2, with the very disadvantageous water vapor condition, though CAPE is large and the ascending velocity can also reach 6 m s^{-1} in the stage of descending, sustained for a short time. In Process 3, with large CAPE near to that in Process 1 and ample water vapor in middle levels, the ascending velocity reduces to 3 m s^{-1} after its maximum value in the mature stage of the storm. There are two aspects for why CAPE and water vapor can affect sustained updrafts. Firstly, CAPE, as the energy source of convection, is the base of sustained convection. Secondly, when the water vapor is transferred to the upper level and takes place phase change process, the latent heat is released to heat air, which is in favor of accelerating updrafts. In Process 1, much latent heat is released with ample water vapor being lifted to large height by the strong updrafts, which helps sustain the ascending velocity. In Process 2, the latent heat is less because the large ascending velocity but the scant water vapor, which makes the updraft decrease rapidly. In Process 3, the small ascending velocity leads the condensation process to be slow and more latent heat to be released in low levels. Though released latent heat through phase change from gaseous state to liquid state is smaller than that from gaseous state to solid state, the sufficient water vapor makes the latent heat continuous, and makes the ascending velocity sustained with small value. These analyses explain why the ascending velocity in Processes 1 and 3 can be sustained for a long

time, the ascending velocity in Process 2, however, rapidly decreases to be equivalent to the falling velocity.

In summary, it is found that ascending velocity and water vapor are direct factors affecting lightning activities. Furthermore, ascending velocity and water vapor influence each other. The favorable condition for strong lightning activities is strong and sustainable updrafts, suitable humidity in middle levels, and large humidity in low levels. So far as stratification parameters are concerned, small convective instability index (negative value indicates instability), large CAPE, suitable CIN, large potential equivalent temperature at 700 hPa, and suitable average humidity in the region between 700 and 400 hPa are in favor of strong lightning activities.

6. Conclusions

Three stratifications resulting in different thunderstorms are analyzed by using model in this paper and some conclusions are obtained:

(1) The direct factors affecting the dynamic and microphysical processes of storms and lightning activities are ascending velocity and water vapor.

a) The magnitude of ascending velocity determines when the storm reaches its mature stage and how strong the storm is. Strong updrafts help cloud reach a large height in a short time. The combination of sustained updrafts and sufficient water is in favor of prolonging the mature stage of storm and boosting up lightning activities.

b) Through influencing the generation and persistence of the hydrometeors, especially the hydrometeors that are of important action on electrification process, ascending velocity and water vapor influence the lightning activities. In the condition of strong ascending velocity and ample water vapor, more ice phase hydrometeors will be continuously produced, which will help form large charge density. In the condition of strong ascending velocity and the disadvantageous condition of water vapor, more ice phase hydrometeors

can also be produced temporarily, however, it is difficult for them to be generated largely and persistently. Warm cloud process in which ice phase particles are lack and lightning activities are weak is associated with weak updrafts and enough water vapor.

(2) Ascending velocity and water vapor influence each other and are commonly controlled by stratification.

a) Convective instability index is of indicative action on ascending velocity to a certain extent. Smaller convective instability index which is associated with small humidity in the middle levels indicates large ascending velocity. Small humidity in the middle levels, however, is not in favor of the generation of ice phase hydrometeors. Therefore, strong lightning activities need suitable water vapor conditions in the middle levels.

b) The combination of CAPE and CIN is of important impact on the size of ascending velocity. Large CAPE and suitable CIN are in favor of convection.

c) Updraft is influenced by CAPE and latent heat. Large CAPE and more latent heat are in favor of the persistence of updraft. At the same time, latent heat is influenced by ascending velocity and water vapor commonly.

(3) So far as instable parameters in favor of strong lightning activities are concerned, convective instability index should be smaller than -10°C (negative means instable), the convective available potential energy should be larger than 1000 J kg^{-1} , the convective inhibition should be larger than 40 J kg^{-1} , the 700-hPa potential equivalent temperature should be larger than 340 K and the humidity in the middle levels (700–400 hPa) should be between 35% and 85%.

Furthermore, the relationship between latent instability index and lightning activities and that between lifted index and lightning activities are not shown in this paper. Although these two parameters can act as warning factors for instable stratification, there is no apparent indicative function on the strength of lightning activities.

REFERENCES

- Colson, D., 1960: High level thunderstorms of July 31–August 1, 1959. *Mon. Wea. Rev.*, **88**, 279–285.
- Gardiner, B., D. Lamb, R. L. Pitter, J. Hallett, and C. P. R. Saunders, 1985: Measurements of initial potential gradient and particle charges in a Montana summer thunderstorm. *Journal of Geophysical*, **90**(D4), 6079–6086.
- Gunn, R., and G. D. Kinzer, 1949: The terminal velocity of all for water droplets in stagnant air. *Journal of Meteorology*, **6**, 243–248.
- Guo Fengxia, Zhang Yijun, Qie Xiushu, and Yan Muhong, 2003: Numerical simulation of different charge structures in thunderstorm. *Plateau Meteorology*, **22**(3), 268–274. (in Chinese)
- Guo Fengxia, Zhang Yijun, Yan Muhong, and Dong Wansheng, 2004: The effect of environment temperature and humidity stratification on charge structure in thunderstorms. *Plateau Meteorology*, **23**(5), 678–683. (in Chinese)
- Holton, J. R., 1972: *An Introduction to Dynamical Meteorology*. Academic Press, 319 pp.
- Hu Zhijin and He Guanfang, 1987: Numerical simulation of microprocesses in cumulonimbus clouds. I: Microphysical model. *Acta Meteorologica Sinica*, **45**(4), 467–484. (in Chinese)
- Jorgensen, D. P., and M. A. LeMone, 1989: Vertically velocity characteristics of oceanic convection. *Journal of the Atmospheric Sciences*, **46**(5), 621–640.
- Ma Ming, 2004: A study of the relationship between lightning activities and climate change. Doctoral Dissertation, University of Science and Technology of China. (in Chinese)
- Mansell, E. R., D. MacGorman, C. L. Ziegler, and J. M. Straka, 2002: Simulated three dimensional branched lightning in a numerical thunderstorm model. *Journal of Geophysical Research*, **107**(D9), 4075, doi: 10.1029/2000JD000244.
- Petersen, W. A., S. A. Rutledge, and R. E. Orville, 1996: Cloud-to-ground lightning observations from TOGA COARE: Selected results and lightning location algorithms. *Mon. Wea. Rev.*, **124**(4), 602–620.
- Qie Xiushu, Zhang Yijun, and Zhang Qilin, 2005: Study on the characteristics of lightning discharges and the electric structure of thunderstorm. *Acta Meteorologica Sinica*, **63**(5), 646–658. (in Chinese)
- Randell, S. C., S. A. Rutledge, R. D. Farley, and J. H. Helsdon Jr, 1994: A modeling study on the early electrical development of tropical convection: Continental and oceanic (monsoon) storms. *Mon. Wea. Rev.*, **122**(8), 1852–1877.

- Rutledge, S. A., E. R. Williams, and T. D. Kennan, 1992: The down under Doppler and electricity experiment(DUNDEE): Overview and preliminary results. *Bulletin of the American Meteorological Society*, **73**(1), 3–16.
- Sheng Peixuan, Mao Jietai, and Li Jianguo, 2003: *Atmospheric Physics*. Peking University Press, 304 pp. (in Chinese)
- Sun Anping, Yan Muhong, Zhang Yijun, and Zhang Hongfa, 2002: Numerical study of thunderstorm electrification with a three-dimensional dynamics and electrification coupled model. II: Mechanism of electric structure. *Acta Meteorologica Sinica*, **60**(6), 732–739. (in Chinese)
- Wang Qian and Hu Zhijin, 1990: Three-dimensional elastic atmospheric numerical model and the simulations of a severe storm case. *Acta Meteorologica Sinica*, **48**(1), 467–484. (in Chinese)
- Watson, A. L., R. L. Holle, R. Ortize, and J. R. Nicholson, 1991: Surface wind convergence as a short-term predictor of cloud-to-ground lightning at Kennedy Space Center. *Wea. and Forecasting*, **6**(1), 49–64.
- Williams, E. R., S. A. Rutledge, S. G. Geotis, N. Renno, E. Rasmussen, and T. Rickenbach, 1992: A radar and electrical study of tropical “hot towers”. *Journal of the Atmospheric Sciences*, **49**(15), 1386–1395.
- Wu Baojun and Wang Wenxiu, 1987: *Physical calculation method used in grassroots stations of ocean and meteorology*. Ocean Press, 1–16 and 30–40. (in Chinese)
- Yan Muhong, Liu Xincheng, and An Xuemin, 1996a: A simulation study of non-inductive charging mechanism in thunderstorm. I: Effect of cloud factor. *Plateau Meteorology*, **15**(4), 425–437. (in Chinese)
- Yan Muhong, Liu Xincheng, and An Xuemin, 1996b: A simulation study of non-inductive charging mechanism in thunderstorm. II: Effect of environmental factor. *Plateau Meteorology*, **15**(4), 438–447. (in Chinese)
- Yu Dawei, He Guanfang, and Zhou Yong, 2001: Three-dimensional convective cloud seeding model and its field application. *Journal of Applied Meteorological Science*, **12**, 122–132. (in Chinese)
- Yuan Tie and Qie Xiushu, 2005: Seasonal variation of lightning activities and related meteorological factors over the central Qinghai-XiZang Plateau. *Acta Meteorologica Sinica*, **63**(1), 123–127. (in Chinese)
- Zhang Xixuan, 1980: Method of forecasting hail. *Meteorological Monthly*, **4**, 14–15. (in Chinese)
- Zhang Yijun, Yan Muhong, Zhang Cuihua, and Liu Xincheng, 2000: Simulating calculation of charge structure in thunderstorm for different areas. *Acta Meteorologica Sinica*, **58**(5), 617–627. (in Chinese)
- Zheng Dong, Zhang Yijun, Lu Weitao, and Meng Qing, 2005: Atmospheric instability parameters and forecasting of lightning activities. *Plateau Meteorology*, **24**(2), 196–203. (in Chinese)
- Ziegler, C. L., and D. R. MacGorman, 1994: Observed lightning morphology relative to modeled space charge and electric field distributions in a tornadic storm. *Journal of the Atmospheric Sciences*, **51**(6), 833–851.
- Zipsper, E. J., 1994: Deep cumulonimbus cloud systems in the tropics with and without lightning. *Mon. Wea. Rev.*, **122**(8), 1837–1851.